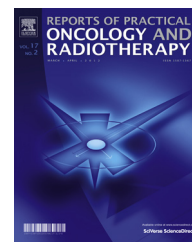


Available online at www.sciencedirect.com

SciVerse ScienceDirect

journal homepage: <http://www.elsevier.com/locate/rpor>

Original research article

Measurement verification of dose distributions in pulsed-dose rate brachytherapy in breast cancer



Patrycja Mantaj^{a,*}, Grzegorz Zwierzchowski^{b,c,1}

^a The Greater Poland Cancer Centre, Department of Radiation Protection, Garbary 15, 61-866 Poznań, Poland

^b The Greater Poland Cancer Centre, Department of Medical Physics, Garbary 15, 61-866 Poznań, Poland

^c Poznan University of Medical Sciences, Department of Electroradiology, Poznań, Poland

ARTICLE INFO

Article history:

Received 28 July 2011

Received in revised form

29 November 2012

Accepted 9 March 2013

Keywords:

Pulse brachytherapy

Implant

Thermoluminescent detectors

Gafchromic EBT dosimetry

ABSTRACT

Aim: The aim of the study was to verify the dose distribution optimisation method in pulsed brachytherapy.

Background: The pulsed-dose rate brachytherapy is a very important method of breast tumour treatment using a standard brachytherapy equipment. The appropriate dose distribution round an implant is an important issue in treatment planning. Advanced computer systems of treatment planning are equipped with algorithms optimising dose distribution.

Materials and methods: The wax-paraffin phantom was constructed and seven applicators were placed within it. Two treatment plans (non-optimised, optimised) were prepared. The reference points were located at a distance of 5 mm from the applicators' axis. Thermoluminescent detectors were placed in the phantom at suitable 35 chosen reference points.

Results: The dosimetry verification was carried out in 35 reference points for the plans before and after optimisation. Percentage difference for the plan without optimisation ranged from –8.5% to 1.4% and after optimisation from –8.3% to 0.01%. In 16 reference points, the calculated percentage difference was negative (from –8.5% to 1.3% for the plan without optimisation and from –8.3% to 0.8% for the optimised plan). In the remaining 19 points percentage difference was from 9.1% to 1.4% for the plan without optimisation and from 7.5% to 0.01% for the optimised plan.

No statistically significant differences were found between calculated doses and doses measured at reference points in both dose distribution non-optimised treatment plans and optimised treatment plans.

Conclusions: No statistically significant differences were found in dose values at reference points between doses calculated by the treatment planning system and those measured by TLDs. This proves the consistency between the measurements and the calculations.

© 2013 Published by Elsevier Urban & Partner Sp. z o.o. on behalf of Greater Poland Cancer Centre.

* Corresponding author. Tel.: +48 618850521; fax: +48 618850723.

E-mail addresses: patrycja.mantaj@wco.pl (P. Mantaj), grzegorz.zwierzchowski@wco.pl (G. Zwierzchowski).

¹ Tel.: +48 6188819.

1. Background

A pulsed-dose rate brachytherapy (PDR) is one of the most commonly used methods of breast cancer treatment, which has been known and applied since the early 1990s. The method employs the isotope ^{129}Ir with initial activity of 15–37 GBq (0.5–1.0 Ci) and dose rate of 0.5–1.0 Gy/h. An essential part of this method is the obtaining of a proper dose distribution around an implant (or implants). Those distributions can be derived from dose distribution optimisation algorithms used by IT treatment planning systems. They require, however, a precise dosimetric verification in order to ensure a high quality of treatment and patient safety.^{9–13,15,23–26}

2. Aim

The aim of the study was to compare measured doses with thermoluminescent detectors and calculated by the Plato treatment planning system for treatment plans before and after the optimisation.

3. Material

3.1. Tissue-like phantom

A permanent phantom was made to establish dose distributions; it was constructed from a mixture of wax and paraffin. The material used had a mean atomic number of $Z_m = 6.82$, and a mean density of $\rho_m = 0.9 \text{ g/cm}^3$. It constituted a good approximation of soft tissues, as the properties of the mixture used to build it roughly corresponded to those of water ($Z_m = 6.62$, $\rho_m = 1.0 \text{ g/cm}^3$). The phantom consisted of two parts and both of them were blocks made from a mixture of wax and paraffin, sized $16 \text{ cm} \times 14 \text{ cm} \times 1 \text{ cm}$ (Fig. 1). Four applicators for radiation source were placed centrally in the lower part at 1 cm intervals, and three in the upper part at 1 cm intervals.¹⁵ Thermoluminescent detectors (TLD) were placed on both parts of the phantom to measure doses. The TLDs were placed over the applicators at 2 cm intervals – five TLD per applicator.

3.2. Thermoluminescent detectors

Dose measurements at reference points set with the Plato treatment planning system were made using Harshaw TLD-100 thermoluminescent detectors in the form of lithium fluoride (LiF) sinters sized $3.0 \text{ mm} \times 3.0 \text{ mm} \times 0.9 \text{ mm}$. Dose values were read out by Harshaw 3500 TLD Reader. The detectors were calibrated in a cobalt 60 beam (Theratron 780 radiotherapy unit) with a mean radiation energy of 1.25 MV, radiation field of $20 \text{ cm} \times 20 \text{ cm}$ and prescribed dose of 200 cGy. The calibration process was repeated five times. Each of the detectors was assigned a calibration ratio. The detectors were annealed after each read-out.^{4,11,17,19}

3.3. Dosimetry films

To make a quality verification of dose distributions calculated with the Plato treatment planning system, Gafchromic EBT dosimetry films were used after having been cut down to the size of $75 \text{ mm} \times 75 \text{ mm}$. The insertion of the films into the tissue-like phantom did not distort the density of the medium, as mean density of the film was similar to that of tissues (water). A dose-dependent darkening was visible right after a radiation session as blue tints and shades. The film response, i.e. the dependence of optical density on radiation dose, was linear for a wide range of doses (from approx. 0.1 Gy to 10 Gy). The darkening of a film in this case will depend only on the total dose absorbed during a measurement.^{1–3,5,6,14,16,18–20}

4. Method

4.1. Dose distribution calculations

In the case of pulsed-dose rate brachytherapy, a treatment plan contains information on dose distributions and their corresponding active source dwell positions along the applicator and source dwell times in particular positions. The dose distribution thus established depends on the above mentioned parameters and on physical properties of the irradiated medium. The treatment plan in this study was developed using Nucletron Plato v. 14.1.3. planning system. Thirty-five reference points were set. The placement of detectors was verified by an integrated brachytherapy unit (IBU). Received X-ray images were used to set a radiation volume and develop a treatment plan. Each source dwell position was assigned a reference point located 5 mm from each of the applicator axis. Of 119 reference points, 35 were selected (A1–A35) and set at 2 cm intervals along each applicator axis. Thirty-five thermoluminescent detectors were selected based on variation ratio and put at these points (A1–A35). The doses derived with the Plato system were then subjected to dosimetric verification. Then, dose distributions of particular treatment plans (Fig. 2) were optimised and doses verified at reference points. A point optimisation was made, with source dwell positions diversified so that doses received at reference points was equal to a prescribed value.

4.2. Dose distribution measurements

The dosimetric verification of dose distributions for particular plans consisted of two stages. In stage one, doses were measured at reference points for non-optimised treatment plans, while in stage two, they were measured for the optimised ones. The prescribed dose was 3 Gy (6 pulses, 0.5 Gy each). The location of thermoluminescent detectors was identical as the location of the pre-set reference points. In the studied case, the distance covered by the radioactive isotope from the end of the applicator unit to the farthest dwell position was 1159 mm (maximum distance is 1400 mm). The verification of dose distributions for particular treatment plans was also made with EBT dosimetry films. The films were inserted in the phantom after being properly clipped. The darkening distributions of the dosimetry films were recorded in a 16-bit grey scale and

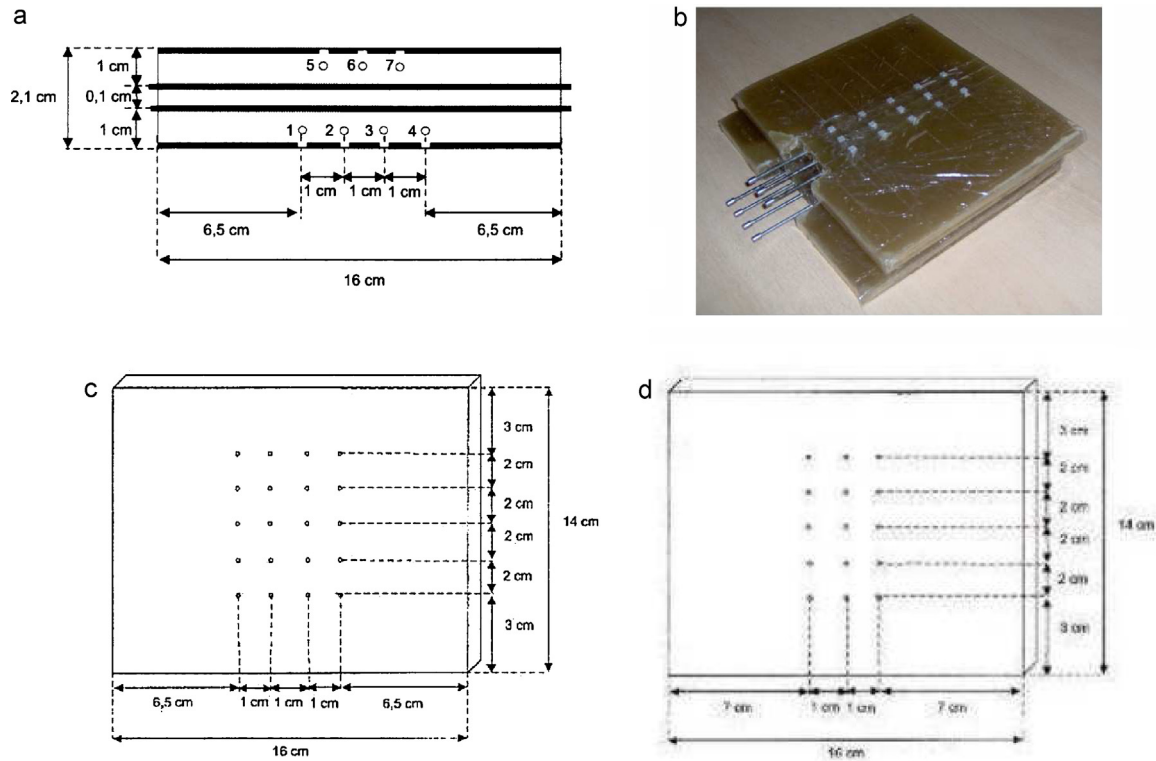


Fig. 1 – The wax and paraffin phantom for dosimetric verification of dose distributions in pulsed-dose rate brachytherapy: (a) a scheme of the phantom, (b) image of the phantom with applicators and thermoluminescent detectors, (c) the lower part of the phantom and (d) the upper part of the phantom.

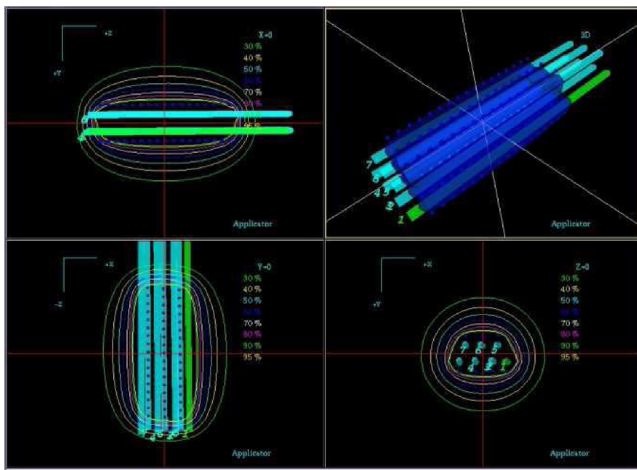


Fig. 2 – A presentation showing isodose distributions for a non-optimized plan developed by the Plato treatment planning system.

then transformed into isodose images by means of Mephisto software.^{7,8}

4.3. Comparison between calculated and measured doses

The Wilcoxon and sign tests were used to compare doses calculated at reference points by the treatment planning

system with those measured by thermoluminescent detectors. These tests are made for two dependent variables. They serve to check the significance of differences between two dependent samples. As its name suggests, the sign test is based on signs of differences between successive pairs of results and, therefore, is used primarily for qualitative comparisons.

5. Results

5.1. Calibration of thermoluminescent detectors

The calibration process was carried out for 50 thermoluminescent detectors. Prescribed dose was 2 Gy. Five series of calibration measurements were made. A measure of dispersion (standard deviation and variation ratio) and a measure of central tendency (arithmetic mean) were calculated for each detector.²⁷ Additionally, each detector was assigned a calibration ratio which allowed to determine absorbed radiation dose. They were defined as follows: where: D_k , value of dose prescribed for the TLD calibration process, \bar{x} mean value derived from detector read-outs.

The results of calibration of thermoluminescent detectors and value of calibration ratio are shown in Table 1. The marked number of TLDs and their ratio mean the detectors used to measurements.

The arithmetic mean with standard deviation is presented in Fig. 3.

Table 1 – TLD calibration measurements and the results of the calibration factor. Marked No., number of detector; \bar{x} , the average arithmetic; SD, standard deviation; ν , coefficient of variation; W_k , calibration factor.

No	Next measurements [μC]					\bar{x} [μC]	SD [μC]	ν [%]	W_k [$\text{Gy}/\mu\text{C}$]
	1	2	3	4	5				
1	5.23	5.15	4.91	4.88	4.99	5.03	0.15	3.04	0.40
2	4.40	2.86	4.27	4.30	4.34	4.03	0.66	16.28	0.46
3	4.11	2.28	4.06	4.13	4.12	3.74	0.82	21.82	0.49
4	4.83	3.07	4.56	4.69	4.42	4.31	0.71	16.49	0.45
5	4.38	4.21	4.16	4.37	4.26	4.27	0.10	2.26	0.47
6	4.56	4.46	4.25	4.47	4.56	4.46	0.13	2.85	0.44
7	4.21	3.99	4.08	4.21	4.26	4.15	0.11	2.66	0.47
8	4.31	4.12	4.06	4.06	2.56	3.82	0.71	18.66	0.78
9	4.82	4.68	4.73	4.54	4.68	4.69	0.10	2.17	0.43
10	5.02	4.85	4.79	3.80	3.87	4.47	0.58	13.03	0.52
11	4.73	4.65	4.65	4.58	4.67	4.66	0.05	1.12	0.43
12	5.23	5.23	4.94	5.01	5.03	5.09	0.13	2.64	0.40
13	5.17	4.93	5.04	4.80	4.92	4.97	0.14	2.87	0.41
14	5.10	5.16	5.03	5.07	5.08	5.09	0.05	0.91	0.39
15	4.90	4.82	4.63	4.52	4.58	4.69	0.16	3.48	0.44
16	4.59	4.72	4.61	4.48	4.60	4.60	0.08	1.81	0.43
17	4.76	4.79	4.73	4.48	4.72	4.70	0.12	2.65	0.42
18	5.20	5.20	4.84	4.69	4.62	4.91	0.28	5.63	0.43
19	4.49	4.59	4.52	4.32	4.31	4.45	0.13	2.82	0.46
20	4.39	4.30	4.20	4.07	4.13	4.22	0.13	3.03	0.48
21	4.91	4.99	4.78	4.78	4.85	4.86	0.09	1.86	0.41
22	4.54	4.75	4.52	4.58	4.59	4.59	0.09	1.97	0.44
23	4.70	4.50	4.44	4.45	4.59	4.54	0.11	2.42	0.44
24	4.93	5.20	5.06	5.06	5.02	5.06	0.10	1.93	0.40
25	4.97	4.86	4.81	4.92	4.90	4.89	0.06	1.20	0.41
26	4.55	4.71	4.33	4.44	4.52	4.51	0.14	3.09	0.44
27	4.86	4.83	4.71	4.64	4.73	4.75	0.09	1.90	0.42
28	4.74	4.67	4.39	4.60	4.51	4.58	0.13	2.94	0.44
29	4.93	4.96	4.91	4.74	4.90	4.89	0.09	1.79	0.41
30	4.28	4.26	4.24	4.29	4.31	4.27	0.03	0.67	0.46
31	4.86	4.77	4.81	4.80	4.69	4.79	0.06	1.33	0.43
32	4.70	4.78	4.61	4.65	4.56	4.66	0.08	1.82	0.44
33	4.88	4.99	4.86	4.86	4.87	4.89	0.05	1.12	0.41
34	4.81	4.80	4.62	4.57	4.53	4.67	0.13	2.83	0.44
35	4.67	4.80	4.55	4.60	4.48	4.62	0.12	2.68	0.45
36	5.05	5.10	4.95	4.68	4.93	4.94	0.16	3.31	0.41
37	4.71	4.75	4.75	4.85	4.78	4.77	0.05	1.06	0.42
38	4.81	4.86	4.60	4.71	4.72	4.74	0.10	2.14	0.42
39	4.85	5.02	4.93	4.89	4.91	4.92	0.06	1.26	0.41
40	3.94	4.77	4.71	4.54	4.54	4.50	0.33	7.30	0.44
41	4.50	4.63	4.52	4.50	4.43	4.52	0.07	1.60	0.45
42	4.71	4.85	4.52	4.69	4.73	4.70	0.12	2.47	0.42
43	4.79	4.69	4.53	4.79	4.80	4.72	0.11	2.38	0.42
44	4.97	4.77	4.72	4.74	4.81	4.80	0.10	2.11	0.42
45	4.63	4.74	4.36	4.50	4.67	4.58	0.15	3.33	0.43
46	4.93	4.75	4.71	4.72	4.77	4.77	0.09	1.87	0.42
47	4.56	4.83	4.76	4.63	4.56	4.67	0.12	2.64	0.44
48	4.37	4.51	4.47	4.44	4.47	4.45	0.05	1.12	0.45
49	4.77	4.51	4.61	4.61	4.62	4.62	0.09	2.03	0.43
50	4.50	4.70	4.63	4.40	4.52	4.55	0.11	2.50	0.44

5.2. Dose measurements at reference points

Out of 50 thermoluminescent detectors, 35 with the lowest variation ratios were selected for preliminary dose measurement. The measurements were made at 35 reference points (A1–A35) in a wax and paraffin phantom using thermoluminescent detectors. Three series of dose measurements were performed. A measure of dispersion and measure of central tendency were established for each reference point. Fig. 4

provides a graphic representation of arithmetic average with standard deviation based on the results of dose measurements at 35 reference points (A1–A35) for non-optimised and optimised treatment plants.

Using the measurement results and calculated statistical measures, dose reference points were set. Table A1 shows the dose designated on the basis of TLD measurements for both treatment plans with and without optimisation. Comparison of mean values of measured doses on the basis

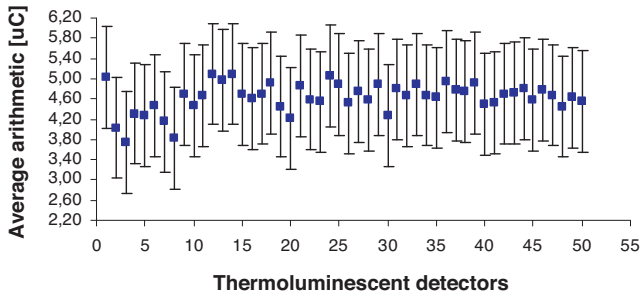


Fig. 3 – Averaged results of thermoluminescent detector calibration with a standard deviation.

of TLD measurements with doses calculated by the Plato treatment planning system is summarised in Table A2. A measure of dispersion was also calculated in the set – standard deviation (SD). Both tables are attached in Appendix. Fig. 5 shows a graphic representation of those results.

The tissue-like phantom for dose distribution measurement in pulsed-dose rate brachytherapy designed and built for the purpose of this study proved to be a useful tool.

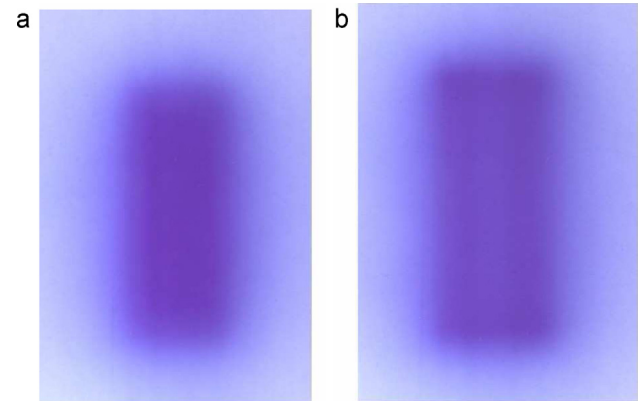
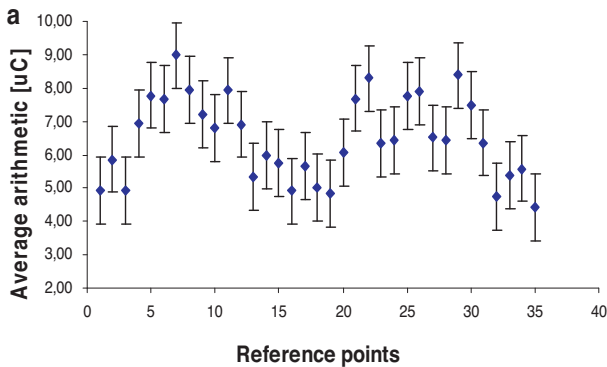


Fig. 6 – Images generated after the irradiation of the EBT dosimetry film: (a) before and (b) after optimisation.

5.3. Dose distribution measurements

Dose distribution verification was also made with Gafchromic EBT dosimetry films. The films were placed in the phantom parallel to the catheter axis. Fig. 5 shows images obtained after the irradiation of the EBT dosimetry film, before and after optimisation. Fig. 6 shows the isodose distribution obtained from the Plato treatment planning system and the isodose

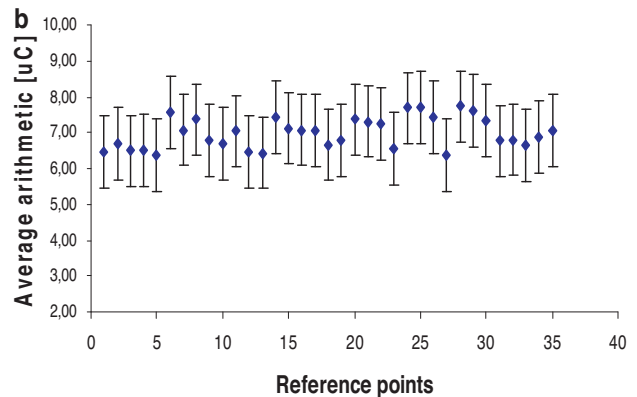


Fig. 4 – Graphic representation of arithmetic average with standard deviation based on the results of dose measurements at reference points for (a) non-optimised and (b) optimised treatment plants.

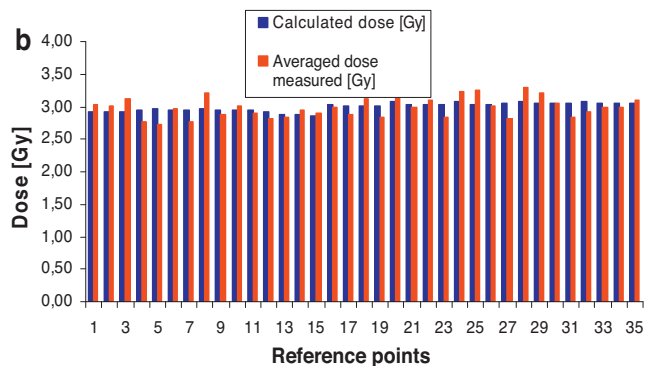
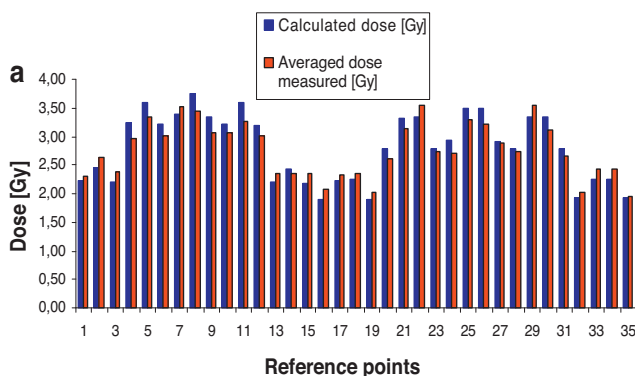


Fig. 5 – Calculated doses and averaged doses measured at 35 reference points for (a) the non-optimised plan and (b) the optimised plan.

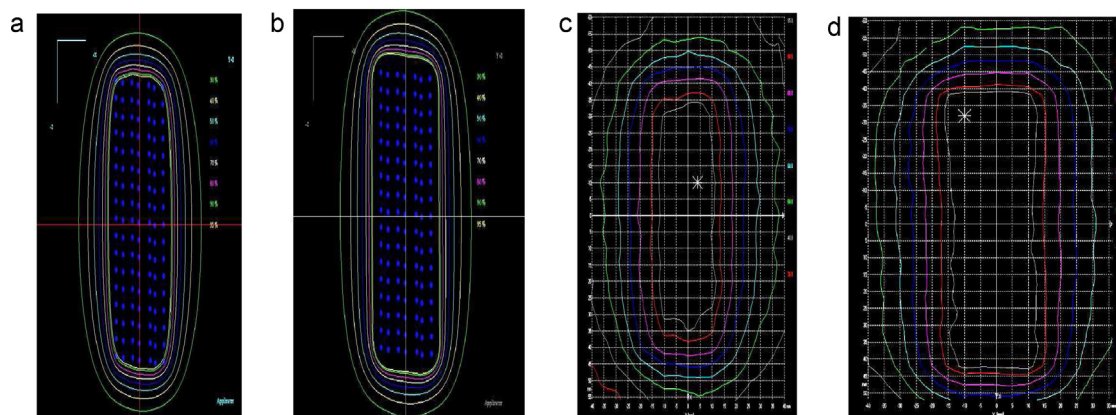


Fig. 7 – Dose distribution received with (a) a non-optimised Plato system, (b) an optimised Plato system, (c) a non-optimised EBT film and (d) an optimised EBT film.

distribution based on the analysis of RBT dosimetry film performed with Mephisto software¹⁸ (Fig. 7).

5.4. Comparison between calculated and measured doses

Doses calculated by the Plato planning system were compared statistically with those measured by thermoluminescent detectors for both non-optimised and optimised treatment plans. The dosimetry verification was performed in 35 reference points for the plans before and after optimisation. For each point, the arithmetic mean, standard deviation (SD) and coefficient of variation were calculated. For the plan without optimisation, in 7 points, the coefficient of variation reached between 5% and 10%, providing a normal variation, while in 28 points, below 4% which indicates a very low volatility. For the optimisation plan, 19 points ranged from 5% to 10% and at 16 points the coefficient of variation reached a value lower than 4% providing a very low volatility, which indicates the precision used in the detectors. Using the results of measurements, the dose in reference points was determined. The values were averaged and the percentage difference between calculated

doses in the treatment planning system and the dose obtained from dosimetric measurements was established. Percentage difference for the plan without optimisation ranged from –8.5% to 1.4% and for the plan with optimisation from –8.3% to 0.01%. For 16 reference points, the percentage difference was negative (for the plan without optimisation from –8.5% to –1.3%, and for the plan with optimisation from –8.3% to 0.8%), which means that the measured dose at these points was smaller than the calculated dose. In the remaining 19 points, percentage difference was positive (for the plan without optimisation from 9.1% to 1.4% and for plan with optimisation from 7.5% to 0.01%) which proving that dose measured at these points was greater than the calculated dose. No statistically significant differences were found in dose values at reference points between doses calculated by the treatment planning system and those measured by TLDs. This proves the consistency between the measurements and the calculations. The results of descriptive statistics are presented in Table 2. The results of statistical verification of compliance of calculated doses by Plato treatment planning system and measured at the points of reference by average of TLD before and after optimisation are presented in Table 3. The analysis

Table 2 – Comparative statistical analysis of the plans before and after optimisation.

Descriptive statistics	Plan without optimisation		Plan with optimisation	
	Plato [Gy]	TLD [Gy]	Plato [Gy]	TLD [Gy]
N	35	35	35	35
Average	2.81	2.77	2.99	2.99
Minimum	1.90	1.94	2.87	2.73
Maximum	3.75	3.55	3.08	3.29
SD	0.59	0.48	0.06	0.15

Table 3 – Results of statistical analysis before and after optimisation. The values of the parameter *p* Wilcoxon test and sign test (Sign test).

A pair of variables tested	Plan without optimisation		Plan with optimisation	
	Level <i>p</i>		Level <i>p</i>	
	Test sign	Wilcoxon	Test sign	Wilcoxon
Plato vs. TLD for 35 N	0.74	0.14	0.74	0.69

used the Sign test and Wilcoxon tests. The results were analysed at the significance level of $\alpha = 0.05$ by means of Statistica 6.0 software.^{19,21,22}

6. Discussion

6.1. Calibration of thermoluminescent detectors

The variation ratio for the 50 thermoluminescent detectors subjected to calibration was very low, indicating small differences in successive measurements, or in other words, high precision of the applied thermoluminescent detectors. Only in four cases were variation ratios higher than 10%, meaning a large variation.

6.2. Dose measurements at reference points

Dosimetric verification was performed at 35 reference points (A1–A35) for treatment plans before and after optimisation. Arithmetic mean, standard deviation (SD) and variation ratio were all calculated for each point. For the non-optimised plans, the variation ratio at seven points came within the range of 5–10%, suggesting a normal variation, and in 28 points it was below 4% signifying a low variation. For the optimised plans, 19 points came within the range of 5–10%, and for 16 points the variation ratio was found to be below 4% meaning a low differentiation of results and high accuracy of the applied detectors. Based on the measurement results, dose sizes at reference points were established. The values thus obtained were averaged and then a percent difference was set between doses calculated in the treatment planning system and those derived from dosimetric measurements. The percent difference for the non-optimised plan was in the range of –8.5% to 1.4%, whereas for the optimised plan it ranged from –8.3% to 0.01%. At 16 reference points, the percent difference was negative (for non-optimised plan: from –8.5% to –1.3%; for optimised plan: from –8.3% to –0.8%), meaning that doses measured at those points were lower than those calculated by the treatment plan. At the remaining 16 reference points, the percent difference was positive (for non-optimised plan: from 9.1% to 1.4%; for optimised plan: from 7.5% to 0.01%), meaning that doses measured at those points were higher than those calculated by the treatment plan. The reason for the existing disparity between the calculated and measured doses may lie in the occurrence of substantial dose gradients in the radiated volume. It may also be caused by differences in the mean density and mean atomic number between the soft tissue (water) and the material the phantom was made of, the phantom being, after all, just an approximation of the conditions inside a patient's body. The existing disparity may also be accounted for by displacements of thermoluminescent detectors in the process of their being placed in the phantom. The phantom also made it possible to verify dose distributions calculated by the Plato treatment plan before and after optimisation. Dosimetric verification was made with Gafchromic

EBT dosimetry films. Qualitative features of isodose distributions for calculated doses were compared with those received from the digitalisation of dosimetry films. Images thus generated enabled a visual comparison of isodose shapes and locations as well as a radiation field marked by those isodoses. The comparison revealed no significant differences between dose distribution calculated by the Plato treatment planning system and that measured by dosimetry films. The result demonstrates that calculation algorithms of the Plato treatment planning system provide reliable dose distributions in planned radiation volumes typical for pulsed-dose rate brachytherapy.

6.3. Comparison between calculated and measured doses

The study employed nonparametric tests for dependent variables: the Wilcoxon test and sign test. Received *p* values were analysed at the statistical significance level of $\alpha = 0.05$. In the case of very small samples (3 measurements), all the results had $p > 5\%$. The received results of $p > 0.05$ do not provide grounds for declining the zero hypothesis, that is the assumption that there are no significant differences in values at reference points between doses calculated by the Plato treatment planning system and those measured with thermoluminescent detectors. The received statistics allow the claim that calculation algorithms of the Plato treatment planning system provide reliable dose distributions in planned target volumes for pulsed-dose rate brachytherapy.

7. Conclusion

The study also confirmed the dosimetric correctness of the algorithm used for calculation of doses in the Plato system in pulsed-dose rate brachytherapy. No statistically significant differences were found between calculated and measured doses and the correctness of the dose distribution optimisation algorithm was verified. No statistically significant differences were found in dose values at reference points between doses calculated by the treatment planning system and those measured by TLDs. This proves the consistency between the measurements and the calculations.

Conflict of interest

None declared.

Financial disclosure

None declared.

Appendix A.

Tables A1 and A2.

Table A1 – Measured doses in 35 of reference points for treatment plans without optimisation and with optimisation.

Reference points	Measured doses [Gy]					
	Without optimisation			With optimisation		
	D_{z1}	D_{z2}	D_{z3}	D_{z1}	D_{z2}	D_{z3}
A1	2.12	2.44	2.34	3.08	3.20	2.80
A2	2.69	2.57	2.63	3.13	2.81	3.09
A3	2.34	2.37	2.41	3.04	3.21	3.13
A4	2.94	2.94	2.98	2.80	2.70	2.81
A5	3.42	3.34	3.26	2.69	2.80	2.71
A6	3.01	2.96	3.08	3.08	2.75	3.08
A7	3.52	3.53	3.53	2.74	2.80	2.79
A8	3.39	3.49	3.48	3.25	3.14	3.22
A9	3.02	3.16	3.03	2.76	3.18	2.72
A10	3.05	3.07	3.07	3.23	2.74	3.04
A11	3.26	3.23	3.29	2.66	3.23	2.80
A12	2.99	3.03	3.01	3.05	2.69	2.71
A13	2.41	2.35	2.32	2.74	3.00	2.77
A14	2.27	2.28	2.54	3.08	2.73	3.01
A15	2.32	2.31	2.40	2.70	3.05	2.98
A16	2.09	2.05	2.05	3.31	2.85	2.78
A17	2.45	2.45	2.05	2.81	2.73	3.13
A18	2.34	2.34	2.34	3.31	2.75	3.29
A19	2.00	2.01	2.05	2.87	2.88	2.75
A20	2.65	2.57	2.59	2.90	3.34	3.24
A21	3.15	3.13	3.15	3.21	2.85	2.89
A22	3.52	3.53	3.61	2.86	3.21	3.26
A23	2.94	2.65	2.64	2.91	2.77	2.81
A24	2.73	2.73	2.64	3.27	3.21	3.18
A25	3.32	3.28	3.23	3.20	3.28	3.27
A26	3.26	3.17	3.22	3.25	2.89	2.92
A27	2.76	3.09	2.79	2.87	2.79	2.80
A28	2.62	2.93	2.65	3.22	3.33	3.31
A29	3.48	3.57	3.61	3.23	3.21	3.22
A30	3.18	3.01	3.16	2.77	3.19	3.19
A31	2.66	2.65	2.68	2.85	2.76	2.89
A32	2.01	2.05	2.05	2.94	2.87	2.93
A33	2.39	2.40	2.47	2.76	3.23	2.96
A34	2.41	2.40	2.44	2.88	3.25	2.81
A35	2.02	1.78	2.02	3.22	2.88	3.22

Table A2 – The average measured dose and calculated dose metrics in 35 reference points for treatment plan optimisation and without optimisation. Marked \bar{D}_z , average measured dose; \bar{D}_o , calculated dose; SD, standard deviation; R, percentage difference.

Reference points	Without optimisation				With optimisation			
	\bar{D}_z [Gy]	\bar{D}_o [Gy]	SD [Gy]	R [%]	\bar{D}_z [Gy]	\bar{D}_o [Gy]	SD [Gy]	R [%]
A1	2.30	2.23	0.16	-3.31	3.03	2.92	0.21	-3.73
A2	2.63	2.46	0.06	-7.06	3.01	2.93	0.17	-2.57
A3	2.37	2.21	0.04	-7.33	3.12	2.92	0.08	-7.17
A4	2.95	3.24	0.02	8.83	2.77	2.95	0.06	6.08
A5	3.34	3.60	0.08	7.22	2.73	2.96	0.06	7.80
A6	3.02	3.21	0.06	6.10	2.97	2.95	0.19	-0.79
A7	3.53	3.38	0.01	-4.35	2.78	2.95	0.03	5.66
A8	3.45	3.75	0.06	7.99	3.20	2.96	0.06	-8.29
A9	3.07	3.35	0.08	8.48	2.89	2.94	0.25	1.83
A10	3.06	3.22	0.01	4.91	3.00	2.94	0.24	-2.31
A11	3.26	3.59	0.03	9.11	2.90	2.95	0.30	1.81
A12	3.01	3.20	0.02	5.89	2.82	2.93	0.20	4.02
A13	2.36	2.20	0.05	-7.23	2.84	2.87	0.14	1.13
A14	2.36	2.43	0.15	2.59	2.94	2.89	0.19	-1.66
A15	2.35	2.18	0.05	-7.40	2.91	2.87	0.19	-1.54
A16	2.06	1.90	0.02	-8.54	2.98	3.04	0.29	1.88

Table A2 – (Continued)

Reference points	Without optimisation				With optimisation			
	\bar{D}_z [Gy]	\bar{D}_o [Gy]	SD [Gy]	R [%]	\bar{D}_z [Gy]	\bar{D}_o [Gy]	SD [Gy]	R [%]
A17	2.32	2.24	0.23	−3.48	2.89	3.02	0.21	4.24
A18	2.34	2.25	0.00	−4.30	3.12	3.02	0.32	−3.17
A19	2.02	1.90	0.03	−6.20	2.83	3.01	0.07	5.86
A20	2.60	2.78	0.04	6.48	3.16	3.07	0.23	−3.04
A21	3.14	3.32	0.01	5.45	2.99	3.04	0.20	1.70
A22	3.55	3.33	0.05	−6.62	3.11	3.04	0.22	−2.24
A23	2.74	2.78	0.17	1.37	2.83	3.04	0.07	6.94
A24	2.70	2.93	0.05	7.75	3.22	3.07	0.04	−4.93
A25	3.28	3.49	0.05	6.09	3.25	3.04	0.04	−6.96
A26	3.21	3.50	0.04	8.08	3.02	3.04	0.20	0.72
A27	2.88	2.92	0.18	1.40	2.82	3.05	0.05	7.45
A28	2.73	2.80	0.17	2.28	3.29	3.08	0.06	−6.66
A29	3.55	3.34	0.06	−6.37	3.22	3.05	0.01	−5.59
A30	3.12	3.35	0.09	6.84	3.05	3.05	0.24	0.01
A31	2.67	2.79	0.01	4.58	2.83	3.06	0.07	7.39
A32	2.04	1.91	0.02	−6.37	2.91	3.08	0.04	5.25
A33	2.42	2.25	0.04	−7.38	2.98	3.05	0.24	2.23
A34	2.42	2.26	0.02	−7.04	2.98	3.05	0.23	2.33
A35	1.94	1.91	0.14	−1.32	3.11	3.05	0.20	−1.90

REFERENCES

- Butson MJ, et al. High sensitivity radiochromic film dose comparisons. *Phys Med Biol* 2002;**47**:291–5.
- Butson MJ, Yu PK, Cheung T, Inwood D. Polarization effects on a high sensitivity radiochromic film. *Phys Med Biol* 2003;**48**:207–11.
- Butson MJ, Cheung T, Yu PK. Radiochromic film dosimetry in water phantoms. *Phys Med Biol* 2001;**46**:27–31.
- Cheung T, Butson MJ. Evaluation of a fluorescent light densitometer for radiochromic film analysis. *Radiat Meas* 2002;**35**:13–6.
- Cheung T, Butson MJ. Use of multiple layers of Gafchromic film to increase sensitivity. *Phys Med Biol* 2001;**46**:235–40.
- Dempsey JF, Low DA, Kirov AS, Williamson JF. Quantitative optical densitometry with scanning-laser film digitizers. *Med Phys* 1999;**26**:1721–31.
- Klassen NW, Zwan L, Cygler J. GAFCHROMIC MD-55: investigated as a precision dosimeter. *Med Phys* 1997;**24**:1924–34.
- Łobodziec W. *Dozymetria promieniowania jonizującego w radioterapii*. Katowice: Wydawnictwo Uniwersytetu Śląskiego; 1999.
- Makarewicz R. *Brachyterapia HDR, Via Medica*; 2004.
- Makarewicz R, Fijuth J. Brachyterapia w leczeniu chorych na raka płuca. *Współczesna Onkol* 2002;**6**:37–40.
- Malicki J, Kierkowski J, Kosicka G, Dymicka M, Stryczyńska G. Does in vivo dosimetry improve quality of radiotherapy: evaluation of 1000 patient's checks. *Rep Pract Oncol Radiother* 2001;**6**:35.
- Malicki J, Roszak A, Kosicka G, Jaroszyk S. Effectiveness of "mobile" and stationary X-ray units and compute tomography in brachytherapy treatment planning. *Rep Pract Oncol Radiother* 1998;**3**:9–12.
- Malicki J, Zwierzchowski G, Roszak A. Nowoczesne metody planowania leczenia. *Rep Pract Oncol Radiother* 2000;**1**:25.
- Meigooni AS, et al. Dosimetric characteristics of an improved radiochromic film. *Med Phys* 1996;**23**:1883–8.
- Murawa P, Mańczak M, Wasiewicz J, Gracz A, Bręborowicz D, Malicki J. Lymphatic mapping and sentinel lymph node biopsy in breast cancer in clinical stage T1–T2 NO MO. *Rep Pract Oncol Radiother* 2001;**6**:52.
- Moray SD, Bianchi C, Conte L, Novario R, Bhatt BC. Radiochromic film measurement of anisotropy function for high-dose-rate Ir-192 brachytherapy source. *Phys Med Biol* 2004;**49**:4065–72.
- Niewiadomski T. *Fluorek litu i jego zastosowanie w dozymetrii promieniowania jonizującego*. Warszawa: Ośrodek Informacji o Energii Jądrowej; 1968.
- Niroomand-Rad A, et al. Radiochromic film dosimetry: recommendations of AAPM Radiation Therapy Committee Task Group 55. *Med Phys* 1998;**25**:2093–115.
- Nowak A, Malicki J, Wachowiak J, Kosicka G, Stryczyńska G. Comparison of doses measured by thermoluminescent and semiconductor detectors during total body irradiation at Cobalt-60 and 15 MeV Li accelerator. *Rep Pract Oncol Radiother* 2001;**6**:40.
- Pradhan AS, Quast U. In-phantom response of LiF TLD-100 for dosimetry of ¹⁹²Ir HDR source. *Med Phys* 2000;**27**:1025–9.
- Reinstein L, Gluckman G. Comparison of dose response of radiochromic film measured with He–Ne laser, broadband, and filtered light densitometers. *Med Phys* 1997;**24**:1531–3.
- Reinstein L, et al. Predicting optical densitometer response as a function of light source characteristics for radiochromic film dosimetry. *Med Phys* 1997;**24**:1935–42.
- Rembiela A, Białas B. Brachyterapia HDR w leczeniu nowotworów piersi. *Współczesna Onkol* 2002;**12**:81–8.
- Skowronek J, Wierzbicka M. Brachyterapia w leczeniu nowotworów głowy i szyi. *Postępy w Chirurgii Głowy i Szyi* 2004;**1**:3–14.
- Skowronek J, Zwierzchowski G, Piotrowski T. Pulsed dose rate brachytherapy – describing of a method and a review of clinical applications. *Rep Pract Oncol Radiother* 2001;**6**:197–202.
- Skowronek J, Adamska K, Zwierzchowski G, Liebert W. Pulsed dose rate and high dose rate brachytherapy in treatment of malignant glioma recurrences – preliminary assessment. *Ann Univ Mariae Curie Skłodowska Med* 2001;**VIII**(Suppl):189–98.
- Sobczak M, Statystyka. *Aspekty praktyczne i teoretyczne*. Wydawnictwo Uniwersytet Marii Skłodowskiej-Curie; 2006.